



# Vector - axial vector lattice cross section and valence parton distribution in the pion from a chiral quark model



Wojciech Broniowski<sup>a,b,\*</sup>, Enrique Ruiz Arriola<sup>c</sup>

<sup>a</sup> The H. Niewodniczański Institute of Nuclear Physics, Polish Academy of Sciences, 31-342 Kraków, Poland

<sup>b</sup> Institute of Physics, Jan Kochanowski University, 25-406 Kielce, Poland

<sup>c</sup> Departamento de Física Atómica, Molecular y Nuclear and Instituto Carlos I de Física Teórica y Computacional, Universidad de Granada, E-18071 Granada, Spain

## ARTICLE INFO

### Article history:

Received 12 June 2020

Received in revised form 17 August 2020

Accepted 19 September 2020

Available online 22 September 2020

Editor: B. Grinstein

### Keywords:

Valence parton distribution function of the pion

Nambu–Jona-Lasinio model

Good lattice QCD cross sections

Chiral symmetry

## ABSTRACT

Within a chiral quark model, we evaluate the good cross section in the Euclidean space in the vector - axial vector channel, proposed recently by Ma and Qiu as means to extract the so far elusive parton distribution functions of the pion from lattice QCD. Our results are remarkably simple at the quark model scale and agree well, after the necessary QCD evolution, with the most recent lattice calculations at the scale  $\mu \sim 2$  GeV for various values of the lattice pion mass. Comparisons are made as functions of the Ioffe time variable. We also comment on the information on the lowest moments in the momentum fraction  $x$ , generically extractable from such analyses, as well as on the inaccessibility of the  $x \rightarrow 1$  limit from the present data.

© 2020 The Author(s). Published by Elsevier B.V. This is an open access article under the CC BY license (<http://creativecommons.org/licenses/by/4.0/>). Funded by SCOAP<sup>3</sup>.

## 1. Introduction

Hadron structure is most directly visualized in deep inelastic scattering experiments with a typical momentum transfer  $Q \gg 1$  GeV, where the underlying partonic properties or, more specifically, the quark and gluon composition is unveiled at a given resolution wavelength  $\sim 1/Q$ . Due to this fundamental nature, numerous attempts have been made over the last 20 years in order to determine, *ab initio* from QCD, the parton distribution functions (PDFs) and their functional dependence on the momentum fraction carried by the quarks or gluons,  $x$ . What is less known is that this problem was actually faced squarely in the physical Minkowski space in the so-called transverse Hamiltonian lattice approach for the pion [1–3]. For the more popular Euclidean space lattices several computational schemes have been implemented. They range from the early few moments determinations of PDFs [4–7], to the more recent quasi-PDFs [8–11] and pseudo-PDFs [12–21], the lattice cross sections approach [22,23], the LaMET method [24,25], or the Compton Feynman–Hellman approach [26]. The necessary formulation in the Euclidean space, which makes the path integral well defined, hampers direct extractions based on suitable extrap-

olations to the physically accessible Minkowski PDFs. For comprehensive overviews we refer the reader to the white paper [27] and the review [28]. A recent analysis of quasi distributions in the QCD instanton vacuum model was presented in [29].

Whereas these different setups aim to be sufficiently accurate to reliably extract the PDFs at a given scale  $\mu$  and compare them to current phenomenological parameterizations extracted from various experiments at fixed  $Q^2$  values, they in fact propose to calculate different mathematical objects in QCD on the lattice at a given spacing  $a$ . These objects are, however, interesting on their own, since theoretical hadronic models can be directly tested against them after the relevant probing scales are consistently tuned,  $\mu \sim Q \sim 1/a$ , to judiciously represent a similar physical situation.

This is precisely the aim of this paper, where we compare the lattice cross section [22,23] for the pion in the vector - axial vector channel,  $\sigma_{VA}$ , obtained in [30,31], to the results of the Nambu–Jona-Lasinio (NJL) model followed with the leading-order (LO) DGLAP [32–34] evolution. In general, the lattice cross sections, following the early proposal of [35], are a broad class of objects suited for lattice studies, with the following features described by Ma and Qiu [22]: they are calculable in the Euclidean lattice QCD, have a well-defined continuum limit, and share the same and factorizable logarithmic collinear divergences as PDFs. Our comparison, made for  $\sigma_{VA}$  at LO as a function of the Ioffe-time, shows a comfortable agreement within the error bars in the

\* Corresponding author.

E-mail addresses: [Wojciech.Broniowski@ifj.edu.pl](mailto:Wojciech.Broniowski@ifj.edu.pl) (W. Broniowski), [earriola@ugr.es](mailto:earriola@ugr.es) (E. Ruiz Arriola).

whole domain of the lattice data. More generally, we argue that the lattice data for  $\sigma_{VA}$  can be viewed as a determination of the lowest even valence quark moments  $\langle x^n \rangle$ , with satisfactory accuracy up to  $n = 4$ , with no strong sensitivity on the behavior in  $x \rightarrow 1$  region.

Our strategy follows the earlier works on the pion's PDF [36–38], distribution amplitude [39], generalized distribution functions [40], quasi-distribution amplitude [41], quasi- or pseudo-PDFs [42], as well as the double distribution functions [43]. Notably, the pion, which is the pseudo-Goldstone boson of the dynamically broken chiral symmetry in QCD, has many of its properties constrained by low energy theorems. However, it is most challenging from the point of view of lattice QCD and achieving the low physical value of the pion mass has always been a tough numerical issue requiring sufficiently large lattice volumes, such that  $e^{-m_\pi V^{1/3}} \ll 1$ . Also, the experimental extractions of its partonic distributions are not direct and require detailed analyses based on QCD factorization. For these reasons, model studies of sophisticated features of the pion, such as the one presented here, are useful in illustrating theoretical ideas and prove helpful to understand the experimental data or the lattice simulations.

## 2. Basic definitions and methodology

We first very briefly review the relevant definitions and establish the notation. The starting point is the so-called *lattice cross-section* introduced in [30]

$$\sigma_{ab}^{\mu\nu}(\xi, p) \equiv \xi^4 \langle \pi(p) | T \{ J_a^\mu(\xi) J_b^\nu(0) \} | \pi(p) \rangle, \quad (1)$$

where  $a, b$  indicate vector ( $V$ ) or axial vector ( $A$ ) currents,

$$\begin{aligned} J_V^\mu(x) &= \bar{q}(x) \gamma^\mu q(x), \\ J_A^\nu(x) &= \bar{q}(x) \gamma^\mu \gamma^5 q(x). \end{aligned} \quad (2)$$

The (Euclidean) coordinate  $\xi$  separates the two current insertions, whereas  $p$  denotes the momentum of the pion. The isospin indices are suppressed for brevity. One should note that actually Eq. (1) describes a two-current correlator in the pion state, thus is a genuine 4-point function.

The Lorentz decomposition of the combination  $\sigma_{VA}^{\mu\nu}(\xi, p) + \sigma_{AV}^{\mu\nu}(\xi, p)$  is antisymmetric in  $\mu\nu$ , with invariant structures multiplying the tensors  $\epsilon^{\mu\nu\alpha\beta} \xi_\alpha p_\beta$  and  $\xi^\mu p^\nu - \xi^\nu p^\mu$  [30]. At LO considered here only the former matters, with the coefficient denoted as  $\sigma_{VA}(\omega, \xi^2, p^2)$ , where  $\omega = p \cdot \xi$  is the Ioffe time [44,45]. It has been shown in Ref. [23] that the following factorization relation holds for  $\xi \Lambda_{\text{QCD}} \ll 1$ :

$$\begin{aligned} \sigma_{VA}(\omega, \xi^2, p^2) &= \int_0^1 \frac{dx}{x} F(x\omega, \xi^2, x^2 p^2; \mu) q_{\text{val}}(x; \mu) \\ &+ \mathcal{O}(\xi^2 \Lambda_{\text{QCD}}^2), \end{aligned} \quad (3)$$

where  $\mu$  is the factorization scale, the valence (non-singlet) PDF of the pion is

$$q_{\text{val}}(x; \mu) = q(x; \mu) - \bar{q}(x; \mu) \quad (4)$$

and  $F$  is a perturbative kernel which at LO and for  $\xi = 0$  is equal to  $x \cos(\omega x)$ , yielding Eq. (35) from [30]:

$$\sigma_{VA}(\omega) = \int_0^1 \frac{1}{\pi^2} \cos(\omega x) q_{\text{val}}(x; \mu). \quad (5)$$

We recognize here the real part of the Ioffe-time distribution (ITD) at  $\xi^2 = 0$ . ITD is also a focal point of the pseudo-PDF studies [12–

15,17,20,21,46], hence one finds a link between the two methods. Note that  $q_{\text{val}}(x; \mu)$  is scale dependent, thus becomes a function of the renormalization scale  $\mu$ .

The methodology of [23,30,31] is aimed at effectively inverting Eq. (5) or its NLO version to obtain  $q_{\text{val}}(x; \mu)$  from the lattice data for  $\sigma_{VA}(\omega)|_\mu$ . In contrast, we proceed with Eq. (5) directly, using model PDF of the pion in the integrand and confronting the obtained result to the lattice data for  $\sigma_{VA}(\omega)|_\mu$ .

It is useful to introduce the standard Mellin moments of the valence PDF,

$$\langle x^n \rangle_\mu = \int_0^1 dx x^n q_{\text{val}}(x; \mu). \quad (6)$$

At LO, the dependence on the scale  $\mu$  is deduced from the solution of the DGLAP equations, which becomes very simple for the moments,

$$\langle x^n \rangle_\mu = r^{\gamma_n^{(0)}/2\beta_0} \langle x^n \rangle_{\mu_0}, \quad (7)$$

with the *evolution ratio* defined as

$$r = \frac{\alpha(\mu)}{\alpha(\mu_0)}. \quad (8)$$

Here  $\alpha(\mu) = \frac{4\pi}{\beta_0} / \ln\left(\frac{\mu^2}{\Lambda_{\text{QCD}}^2}\right)$  is the LO running coupling constant,  $\Lambda_{\text{QCD}} = 226$  MeV,  $\beta_0 = \frac{11}{3}N_f - \frac{2}{3}N_c$  ( $N_f = 3$ ), and  $\gamma_n^{(0)}$  are the LO non-singlet anomalous dimensions,

$$\gamma_n^{(0)} = -2C_F \left( -4H_{n+1} + \frac{2}{(n+1)(n+2)} + 3 \right) \quad (9)$$

with  $C_F = 4/3$ , and  $H_{n+1} = \sum_{k=1}^n 1/k$  denoting the harmonic sum. When needed, the PDF can then be reconstructed from the moments by means of an inverse Mellin transform after analytic continuation to the complex  $n$  plane (see, e.g., Ref. [47] for details).

If we proceed by a power series expansion for small  $\omega$ , we get

$$\begin{aligned} \pi^2 \sigma_{AV}(\omega)|_\mu &= \sum_{n=0}^{\infty} \frac{(-\omega^2)^n}{(2n)!} \langle x^{2n} \rangle \\ &= \sum_{n=0}^{\infty} \frac{(-\omega^2)^n}{(2n)!} \langle x^{2n} \rangle_{\mu_0} r^{\gamma_n^{(0)}/2\beta_0}. \end{aligned} \quad (10)$$

This simple formula allows one to determine  $\sigma_{VA}$  at a scale  $\mu$ , provided we know it at a *reference* scale  $\mu_0$ . A typically used assignment of the lattice scale  $\mu \sim 1/a$  yields  $\mu = 2$  GeV for the lattice spacing  $a = 0.1$  fm.

The data for  $\sigma_{AV}$  determined on the lattice and displayed later in Figs. 2 or 4 exhibit a sizable dependence on the Ioffe time  $\omega$ , but simultaneously a very weak dependence on the  $\xi^2$  variable. Actually, the coefficient of the  $\xi^2$  term extracted from a fit where finite volume and pion mass effects are also discerned is compatible with zero. This result is to be expected, as these terms correspond to higher twist contributions which within the operator product expansion are connected to the gluon and quark condensates, with non-vanishing leading contributions starting at  $\mathcal{O}(\xi^4)$ .

## 3. Chiral quark model results

In our analysis we use the pion PDF at the (yet to be determined) quark model scale  $\mu_0$ , obtained from the Nambu–Jona-Lasinio (NJL) model [36–38] or the Spectral Quark Model [48,49], which (in the strict chiral limit of  $m_\pi = 0$ ) yield

$$q_{\text{val}}(x; \mu_0) = 1 \quad \text{for} \quad 0 \leq x \leq 1, \quad (11)$$

such that in the chiral limit we find the simple result

$$\sigma_{VA}(\omega, 0, 0)|_{\mu_0} = \frac{1}{\pi^2} \frac{\sin \omega}{\omega}. \quad (12)$$

Chiral corrections in NJL, which are small for the physical value of  $m_\pi$  and moderate for the values used on the lattice, can be readily evaluated from the formula

$$q_{\text{val}}(x; \mu_0) = \frac{\int d^2 k_\perp \frac{k_\perp^2 + M^2}{[k_\perp^2 + M^2 - m_\pi^2 x(1-x)]^2} \Big|_{\text{reg}}}{\int d^2 k_\perp \frac{1}{k_\perp^2 + M^2} \Big|_{\text{reg}}}, \quad (13)$$

where  $M$  denotes the constituent quark mass due to the dynamical chiral symmetry breaking, and “reg” indicates the suitably chosen regularization, needed to dispose of the hard momenta. We use here the Pauli-Villars regularization as described in [50,51].

The pion PDF extracted from the experimental or lattice data largely differs from Eq. (11), which reflects the disparity of the quark model scale,  $\mu_0$ , and the scale corresponding to the data,  $\mu \sim Q$ . To provide a sensible comparison, as already advocated in Ref. [36,37], one crucially needs to evolve the model results from the scale  $\mu_0$  up to the scale  $\mu$ . For the problems of interest, focusing on moderate values of  $x$ , one can use the DGLAP scheme, which is supposed to work best in the intermediate  $x$  region, with  $x$  neither too close to  $x \rightarrow 0$  nor  $x \rightarrow 1$  (we return to this point in the next section).

In chiral quark models, the valence quarks carry by definition (as the only degrees of freedom) 100% of the pion’s momentum, namely

$$\langle x \rangle_{\mu_0} = 1. \quad (14)$$

This condition can be used to determine numerically the *quark model scale*  $\mu_0$ , if we know the momentum fraction carried by the valence quarks at some other scale  $\mu$ , since with the DGLAP evolution (cf. Eq. (7))  $\langle x \rangle_\mu = r \gamma_1^{(0)/2\beta_0} \langle x \rangle_{\mu_0}$ . Due to the positivity of  $\gamma_1^{(0)} = \frac{64}{9}$ , the evolution ratio  $r$  and  $\langle x \rangle_\mu$  also decreases with  $\mu$ . This simply reflects the fact that some momentum is carried by the radiatively generated gluons. To fix  $\mu_0$ , we adopt the method used in our previous works, taking that at  $\mu = 2$  GeV the valence quarks carry  $47 \pm 2\%$  of the total momentum of the pion, as follows from [52] (see also [53,54]). At LO the scale turns out to be  $\mu_0 = 313_{-10}^{+20}$  MeV, with the corresponding coupling  $\alpha(\mu_0)/2\pi = 0.34(4)$ , and the evolution ratio  $r = 0.15(2)$ .

The result of the evolution for the PDF from the initial condition at  $\mu_0$  provided with Eq. (13) is shown in Fig. 1(a), where we compare the model valence PDF of the pion to the experimental extraction at LO from the E615 Fermilab data [55] at the scale  $\mu = 4$  GeV. We note that the experimental extraction of the pion PDF was recently carried out by [56], as well as within the xFitter framework [57], showing consistency at LO. As we see from Fig. 1(a), the agreement of the model and the data is quite remarkable. We note that the results of [58] obtained in light-front holographic QCD model are not far from ours. The NLO effects are below the 10% correction level [37].

The above discussion obviously suggests proceeding in a similar fashion for  $\sigma_{VA}$ , namely, to implement the QCD evolution on the quark model result and compare to the lattice results. This implies extrapolation to the infinite volume limit on the lattice, but at a finite lattice spacing, embodying the operating resolution at the corresponding wavelength  $a \sim 1/Q$ . In addition, one needs to adjust the pion mass in the model to the lattice values. The effect of such a change of  $m_\pi$  for  $q_{\text{val}}$  is shown in Fig. 1(b) and, as we can see, is visible but moderate for the probed values of  $m_\pi$ .

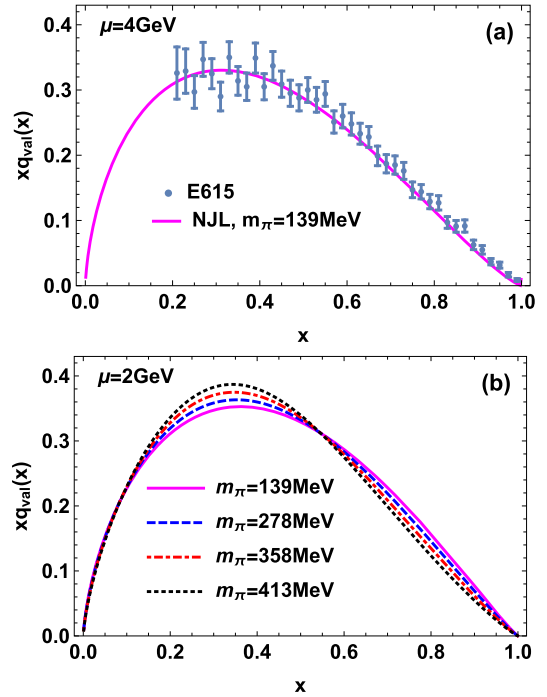


Fig. 1. (a) Valence quark distribution in the NJL model evolved to the scale of 4 GeV corresponding to the E615 Fermilab data (points). (b) LO valence quark distribution in the NJL model (multiplied with  $x$ ) evolved to the scale of 2 GeV corresponding to the lattice simulations, at various values of the pion mass, including those used in [31].

In Fig. 2 we plot  $\sigma_{VA}$  evolved to a high scale for the cases of different  $m_\pi$ . This is effectively performed by fitting the evolution ratio, Eq. (8), to the lattice results. As we can see, the quality of the fits is satisfactory. The corresponding values of  $r$  are displayed on Fig. 3. They are consistent within the error bars, with the lattice data “413L” [31] acceptably away by 2 standard deviations from the mean.

Our weighted fit for the different pion masses allows us to determine the evolution ratio to be  $r = 0.15(1)$ . Using the central value of  $\mu_0 = 313$  MeV, determined in previous works, we infer the lattice scale  $\mu = 2.0(3)$  GeV, which is the same as the value used in [31], and compatible with the lattice spacing  $a \sim 1/\mu \sim 0.1$  fm. We note that using the NLO perturbative kernel given in Eq. (10) of [31], one finds that for the probed values of the separation  $\xi$  this scale is high enough such that the NLO corrections to  $\sigma_{VA}$  are small.

## 4. Generic analysis

### 4.1. Moments content of lattice cross sections

An overall perspective on our study can be obtained from Fig. 4, where we present a combined fit of  $\sigma_{VA}(\omega, \xi^2)$  to all lattice data with NJL model results evolved to the lattice scale of 2 GeV (band). We also show the results of a schematic model with just two moments  $\langle x^2 \rangle$  and  $\langle x^4 \rangle$  treated as free parameters:

$$\sigma_{VA}(\omega) = 1 - \langle x^2 \rangle \omega^2 / 2! + \langle x^4 \rangle \omega^4 / 4!. \quad (15)$$

As we can see, the agreement of the schematic fit with the model is remarkable. It also shows that for the plotted range in the Ioffe time,  $0 \leq \omega \leq 5$ , the corrections to the schematic model from including higher moments,  $\langle x^6 \rangle$ ,  $\langle x^8 \rangle$  etc., are negligible. One may note from Table 1 that taking more moments as free parameters in the schematic fit generates an overfitting effect, with higher

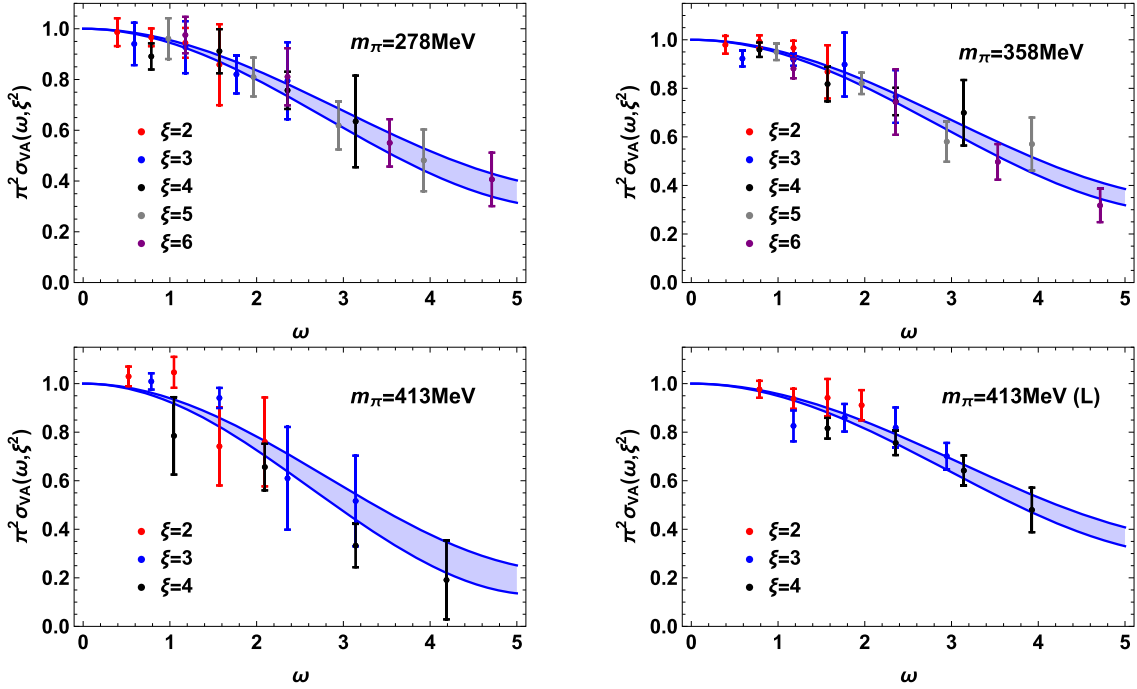


**Fig. 2.** The good lattice cross section  $\sigma_{VA}(\omega, \xi^2)$  from the NJL model evolved to the scale of the lattice data (bands), compared to four sets of the lattice data of [31] (points), plotted as functions of the loffe time  $\omega = p \cdot \xi$ . The width of the band reflects the uncertainty in the lattice data entering the fit of the evolution ratio  $r$ , which is the only adjustable parameter of the model.

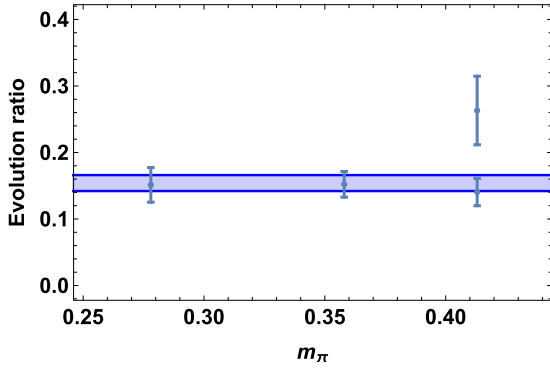


**Fig. 3.** Evolution ratio obtained from fitting the NJL model results to four sets of the lattice data [31] (points) shown in Fig. 2. The band indicates the weighted average with uncertainty reflecting the errors of the data.

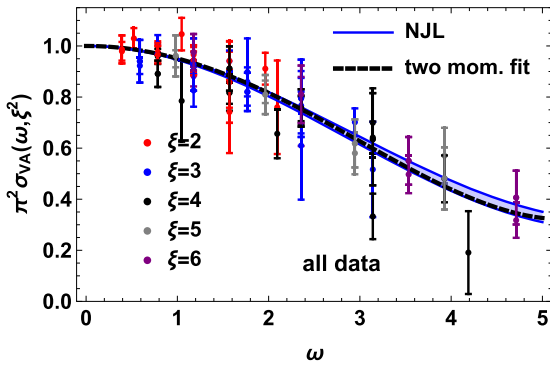


**Fig. 4.** Simultaneous fit of  $\sigma_{VA}(\omega, \xi^2)$  to all lattice data with NJL model results evolved to the lattice scale of 2 GeV (band), and with a schematic model with two moments  $\langle x^2 \rangle$  and  $\langle x^4 \rangle$  treated as free parameters (dashed line).

moments compatible with zero, and increasing errors on  $\langle x^2 \rangle$  and  $\langle x^4 \rangle$ . We note that the values from the schematic model (15) are

**Table 1**

Lowest moment of the valence parton distribution of the pion at the scale 2 GeV, obtained from a simultaneous fit to all lattice samples from [31]. In the NJL model the only free parameter is the evolution ratio, which determines all  $\langle x^i \rangle$  moments. In models labeled “ $m$  mom”, the  $m$  lowest even moments (starting from 2) are treated as independent parameters, while the higher ones are set to zero.

Model	$\langle x^2 \rangle$	$\langle x^4 \rangle$	$\langle x^6 \rangle$	$\langle x^8 \rangle$
NJL	0.106(5)	0.036(2)	0.017(1)	0.010(1)
2 mom.	0.099(7)	0.022(5)	–	–
3 mom.	0.101(12)	0.026(25)	0.005(27)	–
4 mom.	0.102(19)	0.030(77)	0.016(215)	0.018(318)

compatible within uncertainties with the results of [17] obtained from the loffe-time pseudo-PDFs.

Remarkably, the good lattice cross section method generates a stable result for the  $\langle x^2 \rangle$  moment, with an error of the order of a few percent, and also a quite reliable estimate for the  $\langle x^4 \rangle$  moment, with accuracy of 25%, provided higher moments are ignored to avoid the overfitting effect.

#### 4.2. Aspects of the $x \rightarrow 1$ behavior

Recent lattice calculations [59–62] have been undertaken with the hope to settle the long-lasting discussion of the  $x \rightarrow 1$  behavior of the PDF of the pion. The advocated  $\sim (1-x)^2$  behavior in the  $x \rightarrow 1$  limit, found long ago from the QCD counting rules [63], is a feature not manifest in older [55] or newest [57] extractions, and a complete reanalysis (see, e.g., [64]) and/or new experiments remain yet to be done. There are, in particular, renormalization issues regarding elimination of scheme ambiguities [65] which imply the replacement  $\alpha_s(Q^2) \rightarrow \alpha_s(Q^2(1-x))$ , innocuous for  $x \ll 1$  but speeding up the evolution and ultimately hitting the infrared singularity at  $x \rightarrow 1$ . Another more recent scenario concerns the inclusion of the soft-gluon resummation effects [66], which should provide the expected counting rules behavior. The inclusion of these effects in order to extract the PDFs from the Drell-Yan data

should also provide a visible  $(1-x)^2$  behavior in the data (see, e.g., Ref. [67] for a discussion and quantitative comparison).

To shed some light on this point from the lattice perspective, we have tried several  $x \rightarrow 1$  power behaviors fixing the two lowest moments analyzed above to their fitted values and ranging between a good description and a blatant disagreement with the E615 Fermilab experiment [55]. We find that in either case  $\sigma_{AV}$  shows no sensitivity for  $\omega \leq 5$ , in accord with our schematic model analysis. Thus, the insight from the  $\sigma_{VA}$  lattice cross section into the  $x \rightarrow 1$  region would require going to much higher  $\omega$  values. Similar remarks regarding the accessibility of the  $x \rightarrow 1$  limit apply also to other lattice determinations of the pion PDF.

## 5. Conclusions

In this paper we have considered a chiral quark model evaluation of the good cross section in the Euclidean space in the vector - axial vector channel for the pion. Our results, after the necessary QCD evolution (carried out at LO, with next-to leading order analysis left for future work) from the quark model scale to a finer lattice resolution scale  $a$ , display a comfortable agreement with the lattice data in the Ioffe-time region  $\omega \leq 5$ , probed by the lattice simulations at different pion masses [31]. The values of the evolution ratio parameter obtained from our fits are perfectly compatible with our earlier estimations based on other observables, showing the universality of the *quark model + QCD evolution* scheme. Our results also exhibit a weak dependence on the value of the pion mass, in accordance to the lattice studies.

We have also stressed that while the agreement in this particular model case is predetermined by its successful reproduction of the relevant lowest moments of the pion's PDF, the current lattice cross section data would need to be extended well beyond the  $\omega \sim 5$  region to access the  $x \rightarrow 1$  kinematics, which poses a challenge.

An interesting future outlook, both on the lattice and theoretical model sides, would involve analysis of other probing operators in lattice cross sections, such as the energy-momentum tensor, which would provide complementary information on the odd moments of the PDF of the pion.

We cordially thank the authors of [31] for providing us the lattice data from the figures of their paper. We are grateful Michał Praszatałowicz for helpful comments.

This work was supported by the Polish National Science Centre (NCN) Grant 2018/31/B/ST2/01022 (WB), the Spanish Ministerio de Economía y Competitividad and European FEDER funds (grant FIS2017-85053-C2-1-P) and Junta de Andalucía grant FQM-225 (ERA).

## Declaration of competing interest

The authors declare that they have no known competing financial interests or personal relationships that could have appeared to influence the work reported in this paper.

## References

- [1] M. Burkardt, S.K. Seal, Phys. Rev. D 65 (2002) 034501.
- [2] M. Burkardt, S. Dalley, Prog. Part. Nucl. Phys. 48 (2002) 317–362.
- [3] S. Dalley, B. van de Sande, Phys. Rev. D 67 (2003) 114507.
- [4] G. Martinelli, C.T. Sachrajda, Phys. Lett. B 196 (1987) 184–190.
- [5] A. Morelli, Nucl. Phys. B 392 (1993) 518–550.
- [6] C. Best, M. Gockeler, R. Horsley, E.-M. Ilgenfritz, H. Perlt, P.E. Rakow, A. Schafer, G. Schierholz, A. Schiller, S. Schramm, Phys. Rev. D 56 (1997) 2743–2754.
- [7] W. Detmold, W. Melnitchouk, A.W. Thomas, Phys. Rev. D 68 (2003) 034025.
- [8] X. Ji, Phys. Rev. Lett. 110 (2013) 262002.
- [9] J.-W. Chen, S.D. Cohen, X. Ji, H.-W. Lin, J.-H. Zhang, Nucl. Phys. B 911 (2016) 246–273.
- [10] C. Alexandrou, K. Cichy, V. Drach, E. Garcia-Ramos, K. Hadjiyiannakou, K. Jansen, F. Steffens, C. Wiese, Phys. Rev. D 92 (2015) 014502.
- [11] C. Alexandrou, S. Bacchio, K. Cichy, M. Constantinou, K. Hadjiyiannakou, K. Jansen, G. Koutsou, A. Scapellato, F. Steffens, EPJ Web Conf. 175 (2018) 14008.
- [12] A. Radyushkin, Phys. Lett. B 767 (2017) 314–320.
- [13] A. Radyushkin, Phys. Rev. D 96 (2017) 034025.
- [14] K. Orginos, A. Radyushkin, J. Karpie, S. Zafeiropoulos, Phys. Rev. D 96 (2017) 094503.
- [15] C. Monahan, K. Orginos, EPJ Web Conf. 175 (2018) 06004.
- [16] J. Karpie, K. Orginos, S. Zafeiropoulos, J. High Energy Phys. 11 (2018) 178.
- [17] B. Joó, J. Karpie, K. Orginos, A.V. Radyushkin, D.G. Richards, R.S. Sufian, S. Zafeiropoulos, Phys. Rev. D 100 (2019) 114512.
- [18] B. Joó, J. Karpie, K. Orginos, A. Radyushkin, D. Richards, S. Zafeiropoulos, J. High Energy Phys. 12 (2019) 081.
- [19] J. Karpie, K. Orginos, A. Rothkopf, S. Zafeiropoulos, J. High Energy Phys. 04 (2019) 057.
- [20] B. Joó, J. Karpie, K. Orginos, A.V. Radyushkin, D.G. Richards, S. Zafeiropoulos, arXiv:2004.01687, 2020.
- [21] M. Bhat, K. Cichy, M. Constantinou, A. Scapellato, arXiv:2005.02102, 2020.
- [22] Y.-Q. Ma, J.-W. Qiu, Phys. Rev. D 98 (2018) 074021.
- [23] Y.-Q. Ma, J.-W. Qiu, Phys. Rev. Lett. 120 (2018) 022003.
- [24] X. Ji, Sci. China, Phys. Mech. Astron. 57 (2014) 1407–1412.
- [25] J.-H. Zhang, J.-W. Chen, L. Jin, H.-W. Lin, A. Schäfer, Y. Zhao, Phys. Rev. D 100 (2019) 034505.
- [26] A.J. Chambers, R. Horsley, Y. Nakamura, H. Perlt, P.E. Rakow, G. Schierholz, A. Schiller, K. Somfleth, R.D. Young, J.M. Zanotti, Phys. Rev. Lett. 118 (2017) 242001.
- [27] H.-W. Lin, et al., Prog. Part. Nucl. Phys. 100 (2018) 107–160.
- [28] K. Cichy, M. Constantinou, Adv. High Energy Phys. 2019 (2019) 3036904.
- [29] A. Kock, Y. Liu, I. Zahed, arXiv:2004.01595, 2020.
- [30] R.S. Sufian, J. Karpie, C. Egerer, K. Orginos, J.-W. Qiu, D.G. Richards, Phys. Rev. D 99 (2019) 074507.
- [31] R.S. Sufian, C. Egerer, J. Karpie, R.G. Edwards, B. Joó, Y.-Q. Ma, K. Orginos, J.-W. Qiu, D.G. Richards, arXiv:2001.04960, 2020.
- [32] V.N. Gribov, L.N. Lipatov, Sov. J. Nucl. Phys. 15 (1972) 438–450, Yad. Fiz. 15 (1972) 781.
- [33] Y.L. Dokshitzer, Sov. Phys. JETP 46 (1977) 641–653.
- [34] G. Altarelli, G. Parisi, Nucl. Phys. B 126 (1977) 298.
- [35] V. Braun, D. Mueller, Eur. Phys. J. C 55 (2008) 349–361.
- [36] R. Davidson, E. Ruiz Arriola, Phys. Lett. B 348 (1995) 163–169.
- [37] R.M. Davidson, E. Ruiz Arriola, Acta Phys. Pol. B 33 (2002) 1791–1808.
- [38] H. Weigel, E. Ruiz Arriola, L.P. Gamberg, Nucl. Phys. B 560 (1999) 383–427.
- [39] E. Ruiz Arriola, W. Broniowski, Phys. Rev. D 66 (2002) 094016.
- [40] W. Broniowski, E. Ruiz Arriola, K. Golec-Biernat, Phys. Rev. D 77 (2008) 034023.
- [41] W. Broniowski, E. Ruiz Arriola, Phys. Lett. B 773 (2017) 385–390.
- [42] W. Broniowski, E. Ruiz Arriola, Phys. Rev. D 97 (2018) 034031.
- [43] W. Broniowski, E. Ruiz Arriola, Phys. Rev. D 101 (2020) 014019.
- [44] B.L. Ioffe, Phys. Lett. B 30 (1969) 123–125.
- [45] V. Braun, P. Gornicki, L. Mankiewicz, Phys. Rev. D 51 (1995) 6036–6051.
- [46] J. Karpie, K. Orginos, A. Radyushkin, S. Zafeiropoulos, EPJ Web Conf. 175 (2018) 06032.
- [47] E. Ruiz Arriola, Nucl. Phys. A 641 (1998) 461–475.
- [48] E. Ruiz Arriola, W. Broniowski, Phys. Rev. D 67 (2003) 074021.
- [49] E. Ruiz Arriola, W. Broniowski, in: Light-Cone Workshop: Hadrons and Beyond, LC 03, 2003, arXiv:hep-ph/0310044.
- [50] C. Schuren, E. Ruiz Arriola, K. Goeke, Nucl. Phys. A 547 (1992) 612–632.
- [51] E. Ruiz Arriola, Acta Phys. Pol. B 33 (2002) 4443–4479.
- [52] P.J. Sutton, A.D. Martin, R.G. Roberts, W.J. Stirling, Phys. Rev. D 45 (1992) 2349–2359.
- [53] M. Gluck, E. Reya, A. Vogt, Z. Phys. C 53 (1992) 651–656.
- [54] M. Gluck, E. Reya, I. Schienbein, Eur. Phys. J. C 10 (1999) 313–317.
- [55] J.S. Conway, et al., Phys. Rev. D 39 (1989) 92–122.
- [56] P. Barry, N. Sato, W. Melnitchouk, C.-R. Ji, Phys. Rev. Lett. 121 (2018) 152001.
- [57] I. Novikov, et al., arXiv:2002.02902, 2020.
- [58] G.F. de Teramond, T. Liu, R.S. Sufian, H.G. Dosch, S.J. Brodsky, A. Deur, HLFHS, Phys. Rev. Lett. 120 (2018) 182001.
- [59] J. Zhang, J.-W. Chen, L. Jin, H.-W. Lin, Y.-S. Liu, A. Schäfer, Y.-B. Yang, Y. Zhao, PoS LATTICE 2018 (2018) 108.
- [60] J.-W. Chen, H.-W. Lin, J.-H. Zhang, Nucl. Phys. B 952 (2020) 114940.
- [61] T. Izubuchi, L. Jin, C. Kallidonis, N. Karthik, S. Mukherjee, P. Petreczky, C. Shugert, S. Syritsyn, Phys. Rev. D 100 (2019) 034516.
- [62] C. Shugert, X. Gao, T. Izubuchi, L. Jin, C. Kallidonis, N. Karthik, S. Mukherjee, P. Petreczky, S. Syritsyn, Y. Zhao, in: 37th International Symposium on Lattice Field Theory, 2020, arXiv:2001.11650.
- [63] G.R. Farrar, D.R. Jackson, Phys. Rev. Lett. 35 (1975) 1416.
- [64] K. Wijesooriya, P.E. Reimer, R.J. Holt, Phys. Rev. C 72 (2005) 065203.
- [65] S.J. Brodsky, G. Lepage, P.B. Mackenzie, Phys. Rev. D 28 (1983) 228.
- [66] M. Aicher, A. Schafer, W. Vogelsang, Phys. Rev. Lett. 105 (2010) 252003.
- [67] M. Ding, K. Raya, D. Binosi, L. Chang, C.D. Roberts, S.M. Schmidt, Chin. Phys. 44 (2020) 031002.